Journal of Power Sources 196 (2011) 4347–4354

Contents lists available at ScienceDirect

Journal of Power Sources

journal homepage: www.elsevier.com/locate/jpowsour

A comparison between molten carbonate fuel cells based hybrid systems using air and supercritical carbon dioxide Brayton cycles with state of the art technology

D. Sánchez*, J.M. Muñoz de Escalona, R. Chacartegui, A. Muñoz, T. Sánchez

Escuela Técnica Superior de Ingenieros de Sevilla, Camino de los Descubrimientos s/n, 41092 Sevilla, Spain

ARTICLE INFO

Article history:
Received 10 June 2010
Received in revised form 7 September 2010
Accepted 29 September 2010
Available online 7 October 2010

Keywords:
MCFC
Hybrid
Part load
CO_2

ABSTRACT

A proposal for high efficiency hybrid systems based on molten carbonate fuel cells is presented in this paper. This proposal is based on adopting a closed cycle bottoming gas turbine using supercritical carbon dioxide as working fluid as opposed to open cycle hot air turbines typically used in this type of power generators.

First, both bottoming cycles are compared for the same operating conditions, showing that their performances do not differ as much as initially expected, even if the initial objective of reducing compression work is accomplished satisfactorily. In view of these results, a profound review of research and industrial literature is carried out in order to determine realistic specifications for the principal components of the bottoming systems. From this analysis, it is concluded that an appropriate set of specifications must be developed for each bottoming cycle as the performances of compressor, turbine and recuperator differ significantly from one working fluid to another. Thus, when the operating conditions are updated, the performances of the resulting systems show a remarkable advantage of carbon dioxide based systems over conventional air units. Actually, the proposed hybrid system shows its capability to achieve 60% net efficiency, what represents a 10% increase with respect to the reference system.

1. Introduction

Hybrid systems are one of the most interesting applications of high temperature fuel cells, increasing the efficiency of electric power generation by their incorporation into conventional thermal engines, or viceversa. Thus, the high thermal energy (waste heat) stored in the fuel cell exhaust gases is recuperated to produce additional power at the bottoming system (generally a gas turbine). The term "hybrid" comes therefore from the twofold source of useful work production: electrical and thermochemical.

The development of hybrid systems has gone through different stages and, in spite of a number of test plants that have accumulated a large amount of operating hours successfully, there are several technical and economical aspects that must still be resolved before being deployed in distributed generation facilities [1].

Amongst the two most common types of hybrid systems, which are direct integration with pressurised fuel cell and indirect integration with atmospheric fuel cell, this work focuses on systems of the second type. Thus, a comparison is shown in this work for hybrid systems based on atmospheric molten carbonate fuel cells and externally fired/heated gas turbine for which two different working fluids are considered: air and supercritical carbon dioxide. For this latter case, a closed Brayton cycle is adopted.

First, a preliminary analysis of the expected performance of each system under similar operating conditions is presented. Then, an exhaustive review of research and industrial literature is developed in order to establish the expected performance/specifications of each component in the bottoming systems realistically. The outcome of this review is finally used to update the preliminary comparison and conclude which of the bottoming systems is more interesting.

2. Hybrid system. Preliminary analysis

The reference system in this analysis comprises an internal reforming molten carbonate fuel cell whose exhaust gases are used, to heat up the working fluid of the bottoming gas turbine and to preheat the fuel and air feed streams. Finally, the remaining heat content of the exhaust gases is recuperated to generate the steam needed for the natural gas reforming process. It is worth noting that the high water steam content of anodic exhaust gases enables an internal reforming process within the fuel cell, where water steam is supplied by a fraction of these gases that are recirculated to the anode inlet. However, this solution is not used here since it implies a reduction of the heat available for the bottoming cycle and the preheating section. Adding a heat recovery steam

* Corresponding author. Tel.: +34 954 48 64 88; fax: +34 954 48 72 43.
E-mail address: davidsanchez@esi.us.es (D. Sánchez).

0378-7753/$ – see front matter © 2010 Elsevier B.V. All rights reserved.
doi:10.1016/j.jpowsour.2010.09.091

Nomenclature

B	blower
c_p	specific heat at constant pressure (kJ (kg K)$^{-1}$)
h	enthalpy (kJ kg^{-1})
HC	hydrocarbons
HRSG	heat recovery steam generator
HX	heat exchanger
$\dot{m}$	mass flow rate (g s^{-1})
Δp	pressure loss (%)
P	pressure (bar)
ΔT	temperature change (K)
T	temperature (K)
W	specific work (kJ kg^{-1})

Greek letters

ε	effectiveness
γ	specific heat ratio
η	efficiency

generator favours the overall thermal integration and is therefore recommended.

Another interesting issue concerning fuel cell layout is carbon dioxide recirculation. Carbon dioxide is carried in carbonate form from cathode to anode during normal operation of the cell. This transport of carbonate ions is actually the internal flow of charge within the cell and is necessary if electrical work is to be produced. Hence, should carbon dioxide concentration in the cathodic gas drop, the flow of ions would be done at the expenses of the carbonate content of the electrolyte, which would rapidly decrease. This reduction of ionic conductivity of the electrolyte would eventually lead to a dramatic drop in performance of the cell and, therefore, of the complete system [2]. To avoid this situation, a fraction of the exhaust gases from the cell is recirculated back to the cathode inlet. The selection of this recirculation point shown in Fig. 1 is based on the following considerations. First, the molar fraction of carbon dioxide is highest. Second, heat addition to the bottoming cycle is not reduced since the recirculation point is located downstream the high temperature heat exchanger (HX4). Finally, due to this partial cooling of the exhaust gases, the power consumption of the blower (B3) decreases. In this sense, it is worth noting that the temperature of the recirculated stream should not be too low so as to preserve its preheating potential.

For the bottoming cycle in Fig. 1, a conventional externally fired recuperative gas turbine has been adopted. It is well known that one of the major disadvantages of this layout is the rather low turbine inlet temperature that derives from the intermediate temperature of molten carbonate fuel cells and the ineluctable heat losses of heat exchangers. Accordingly, it is expected that realistic turbine inlet temperatures be slightly lower than fuel cell operating temperatures (around 650 °C).

The impact of such low temperatures is studied in reference [3] in detail. Among other minor effects, lower turbine inlet temperature brings about a reduction in turbine work while, at the same time, compressor work remains constant. Consequently, useful work is reduced and, additionally, the impact of pressure losses in the gas turbine is magnified.

To compensate the bottoming cycle for this effect, the authors have previously proposed the utilization of a closed recuperative gas turbine working with supercritical carbon dioxide [4], Fig. 2. The main operating conditions that define this cycle are 75 bar and 35 °C, which is slightly above the critical point (73.77 bar and 30.98 °C). The dramatic drop in compressibility brings about a similar reduction in compressor work while, on the contrary, the turbine works with gas close to ideal behaviour. The different compressibility of the working fluids under consideration is shown in Table 1 where values at compressor/turbine inlet/outlet have been obtained for the reference operating conditions in Table 2. Accordingly, the resulting bottoming system provides higher useful work and is less sensitive to turbine inlet temperature reductions, as explained below. The fundamentals of both cycles, air and supercritical carbon dioxide, are exposed and compared in detail in reference [4] by the authors.

Some aspects of Table 2 are worthy of note. First of all, using carbon dioxide decreases compression work drastically with respect to conventional air cycles, thanks to a much lower compressibility. Hence, in spite of a lower turbine work brought about by a lower specific heat and specific heat ratio ($\gamma = c_p/c_v$) of carbon dioxide, this latter cycle yields 20% higher useful work than the reference case with air. Nevertheless, this increase in useful work does not translate into higher cycle efficiency due to the rather poor performance of carbon dioxide in the recuperator, whose effectiveness is defined in terms of actual to maximum heat exchange as follows [6]:

$$\varepsilon = \frac{\dot{m} \times c_p(T_{\min,\text{out}} - T_{\min,\text{in}})}{\dot{m} \times c_p(T_{\text{hot,in}} - T_{\text{cold,in}})} \quad (1)$$

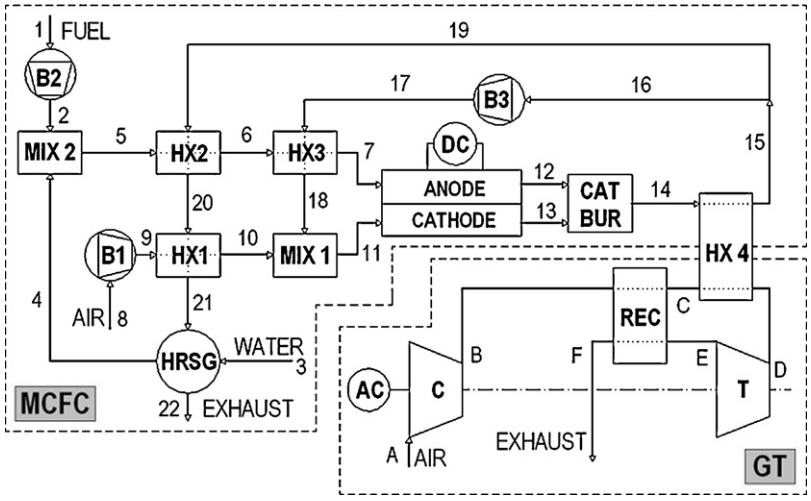

Fig. 1. Reference MCFC–Air hybrid system layout.

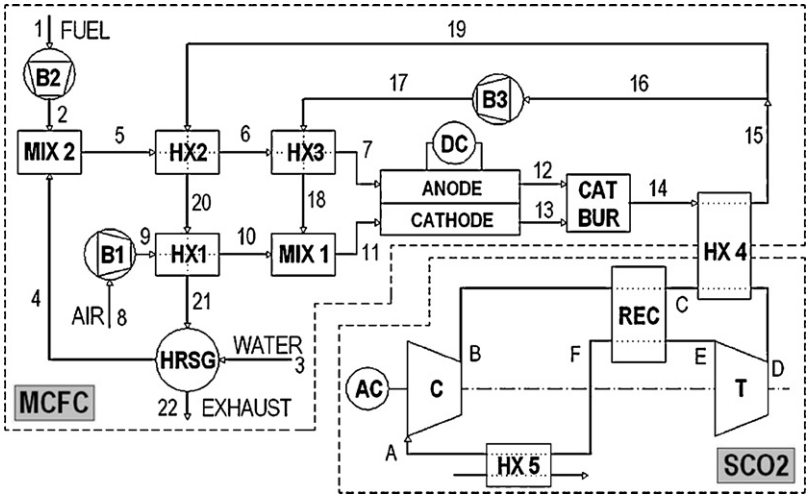

Fig. 2. MCFC–CO_2 hybrid system layout.

Table 1
Compressibility factor.

Location	Variable[a]	Air	CO_2
Compressor inlet	T_r	2.259	1.014
	P_r	0.027	1.017
	Z	1	0.25
Compressor outlet	T_r	3.294	1.271
	P_r	0.080	3.050
	Z	1	0.60
Turbine inlet	T_r	6.994	3.037
	P_r	0.077	2.929
	Z	1	1.02
Turbine outlet	T_r	5.588	2.609
	P_r	0.027	1.059
	Z	1	1

[a] Reduced variables are calculated with respect to critical pressure/temperature for carbon dioxide and pseudo critical pressure/temperature for air, as indicated in [5]. Z is calculated with the generalised compressibility diagram.

Heat exchanger effectiveness as defined in Eq. (1) can be further simplified if the same fluid flows through both sides, hot and cold, at the same mass flow rate:

$$\varepsilon = \frac{T_{\text{cold,out}} - T_{\text{cold,in}}}{T_{\text{hot,in}} - T_{\text{cold,in}}} \tag{2}$$

This definition of effectiveness is admissible for air as it presents an ideal behaviour for the pressure and temperature ranges of interest and, therefore, its specific heat is the same in both sides of the equipment. However, even though carbon dioxide satisfies both of the conditions indicated before, Eq. (2) cannot be used. The reason is that the properties of carbon dioxide are very sensitive to pressure and temperature in the vicinity of the critical point and, therefore, in spite of mass flow rate being the same at both sides of the recuperator, the corresponding specific heats of hot and cold streams are different: $c_p = 1.126\ \text{kJ}\,(\text{kg K})^{-1}$ at hot stream inlet and $c_p = 1.344\ \text{kJ}\,(\text{kg K})^{-1}$ at cold stream inlet.

Looking back at Table 3 again, it can be seen that the potential for waste heat recuperation, considered as the temperature difference between turbine exhaust and compressor discharge, is much higher for carbon dioxide than for air, 400 K and 300 K respectively. However, carbon dioxide cannot take full advantage of this, even if heat exchanger effectiveness is the same as for air, and CO_2 leaves the high pressure side of the recuperator 15 K colder than air in spite of the much higher, 70 K, turbine exhaust temperature. Accordingly, efficiency hardly varies from one cycle to another.

In light of these results, two aspects of carbon dioxide and air cycles must be discussed further. Thus, even though efficiency has not increased significantly with the adoption of a supercritical carbon dioxide cycle, the objective of reducing compression work has been fully accomplished. This is clearly expressed by the so-called useful to expansion work ratio, Table 2:

$$\Phi = \frac{\text{Useful work}}{\text{Expansion work}} = \frac{W_{\text{turb}} - W_{\text{comp}}}{W_{\text{turb}}} = \frac{W_{\text{turb}} - W_{\text{comp}}}{W_{\text{turb}}} \tag{3}$$

The second aspect that must be discussed before arriving to definite conclusions is whether or not the operating conditions in Table 2 are correct. In other words, both cycles, air and carbon dioxide, have been compared when working with the same boundary conditions and internal efficiencies. The first assumption is valid as the maximum and minimum cycle temperatures are constrained by fuel cell operating temperature and ambient temperature. On the contrary, internal efficiencies of major components depend on state of the art technology for each cycle and the particular features of each working fluid, as already discussed for the recuperator. For these reasons, the next section provides the results of a thorough research and industrial literature survey with regard to component

Table 2
Reference operating conditions.

	Air	CO_2
Turbine inlet temperature (K)	923	
Pressure ratio (–)	3:1	
Recuperator effectiveness (%)	85	
Compressor isentropic efficiency (%)	85	
Turbine isentropic efficiency (%)	90	
Compression work (kJ kg^{-1})	130.0	45.0
Expansion work (kJ kg^{-1})	217.3	150.5
Useful work (kJ kg^{-1})	87.3	105.5
Useful to expansion work ratio (%)	40.2	68.3
Gross efficiency (%)	33.0	33.2

Table 3
Heat balance for the operating conditions in Table 2.

Variable	Cycle	A	B	C	D	E	F
P (bar)	Air	1	3	2.94	2.881	1.02	1
	CO_2	75	225	220.5	216.1	78.09	76.53
T (K)	Air	25	153.7	409.4	650	453.4	199.8
	CO_2	35	113.1	395	650	520	172.6
h (kJ kg^{-1})	Air	298.4	428.4	695.2	959.7	742.4	475.7
	CO_2	−109	−64.05	335.1	652.6	502.1	103

Table 4
Technology review (all parameters show percentage values).

Parameter	Cycle	Min	Ave	Max	References
η_C	Air	66	80	85	[7,11–13,15–20,22–32,37]
	CO_2	80	85	91	[38–44,46–49,53]
η_T	Air	78	85	90	[7,11–13,16–20,22–32,37]
	CO_2	85	90	94	[38–39,44,48]
ε_R	Air	78	90	92	[7–10,12,14,17–21,24–25,27,30–31,33–37]
	CO_2	95	95	98	[38,41,44–48,50–52]
$\Delta p_{R,cold}$	Air	2	2.5	3	[7,11,13–14,18,30,35–37]
	CO_2	0.25	0.5	0.66	[42,44–45,47]
$\Delta p_{R,hot}$	Air	3	4.5	6	[7,11,13–14,18,30,35–37]
	CO_2	1.1	1.5	2	[44–45,47]
$\Delta p_{Precooler}$	CO_2	1	1	1	[44–45]

Table 5
Reference operating conditions and hybrid system performance.

Parameter	Unit	AIR	SCO_2
MCFC			
Current density	$A\,m^{-2}$	1100	
Area	m^2	650	
Pressure/temperature	$bar\,K^{-1}$	1/923	
U_f	%	75	
U_{CO_2}	%	70	
Efficiency	%	50.5	
Net power	kW	500	
Bottoming system			
Efficiency	%	26.6	39.9
Power	kW	86.7	129.9
Hybrid system			
Net efficiency	%	55	59.4
Net power	kW	540.4	583.6
GT contribution	%	14.8	20.6

efficiency and gives further information about the validity of the results reported previously.

3. Technology review

A wide literature review has been carried out with the aforementioned objective of determining realistic performance specifications of major components in a gas turbine cycle working with either air or carbon dioxide. A summary of the most relevant results is shown in Table 4. Three different values are given for each parameter along with the main references where they are reported: minimum, maximum and average. The two first values set the lower and upper limit of the corresponding parameter for state of the art technology in similar applications, as quoted in literature. The average values indicated in Table 4 are weighed by the number of times that each value is reported in the references given. Therefore, average values are not necessarily the arithmetic mean between minimum and maximum limits.

Table 4 provides information about compressor/turbine isentropic efficiencies and recuperator effectiveness and pressure losses at both sides, hot and cold; pressure loss at the precooler of the carbon dioxide gas turbine is also reported. From the given values, an immediate conclusion is that the very different properties of the working fluids at the reference operating conditions have an important impact on expected cycle performance. Thus, carbon dioxide seems to be favoured by higher efficiencies and, very important, lower pressure losses. In this regard, it is also worth noting that the recuperator achieves higher effectiveness with carbon dioxide thanks to a higher heat exchange coefficient. The difference in recuperator effectiveness is therefore considered of special importance since this was one of the weakest features of the CO_2 cycle shown in previous sections.

Thus, after the data in Table 4, it is absolutely necessary to update the reference operating conditions in Table 2 with this information and proceed with a new cycle analysis and comparison. This is done in the following section.

4. Hybrid system analysis with updated bottoming systems

The information shown in Table 4 is now used to update air and carbon dioxide bottoming gas turbines, which are then incorporated into the molten carbonate fuel cell following the integration scheme shown in Figs. 1 and 2. The performances of both systems are calculated for a reference operating set point of the fuel cell. These reference conditions and the most relevant performance parameters of both hybrid systems are shown in Table 5, where fuel cell and bottoming system are supposed to operate on a master-slave configuration; i.e. the fuel cell is not affected by the type of gas turbine used in the bottoming system. Tables 6 and 7 show detailed information about pressure, temperature, mass flow rate and composition at each relevant location of air and carbon dioxide systems respectively, following the notation in Figs. 1 and 2.

Some very interesting aspects of Table 5 must be noted, especially the fact that the narrow differences observed in Table 1 are now magnified when realistic specifications for state of the art technology are used. Accordingly, the carbon dioxide bottoming cycle is now 13 percentage points more efficient than that with air, what translates into 50% more power being produced by the former with respect to the latter.

The effect on the hybrid system is an increase in net efficiency from 55% for the conventional MCFC–Air unit to about 60% for the new MCFC–SCO_2 system. The relevance of this performance enhancement can be evaluated from two different angles:

1. Net efficiency increases 10 percentage points with respect to stand alone molten carbonate fuel cells. This is a 20% relative increase.
2. Net efficiency increases 5 percentage points with respect to conventional MCFC–Air systems. This is a 10% relative increase.

Whichever interpretation is adopted, it is confirmed that the newly proposed carbon dioxide based hybrid system is able to achieve 60% net efficiency, a milestone value for state of the art systems based on atmospheric fuel cells.

Finally, a last aspect of Table 5 that deserves attention is the contribution of the bottoming system to power generation. Hence, while hot air turbines hardly generate 15% of total net power, the bottoming system based on carbon dioxide contributes with 20% of the global generation capacity.

Figs. 3–10 show a sensitivity analysis of air and carbon dioxide based systems with respect to the parameters studied in Table 4. Solid and dashed lines are found in all these plots. Solid lines are limited by the lower and upper limits of the parameter under consideration, with the average value marked by a circle. Dashed lines are trend lines, should a parameter take values above or below its upper and lower limits respectively. In all cases, results are shown for air and supercritical carbon dioxide.

With respect to isentropic efficiency of compressor and turbine, it is easily observed that carbon dioxide is less sensitive than air, especially at the compressor, either at system or bottoming cycle level. Hence, carbon dioxide bottoming system efficiency, η_{SCO_2}, only decreases from 42% to 35% when turbine efficiency drops from 93% to 78%, as opposed to the hot air turbine whose efficiency changes from 33% to 21%. This is a twofold difference that is even higher when the compression process is studied. In this case, the sensitivity of η_{Air} to compressor isentropic efficiency is four times higher than that of carbon dioxide.

Table 6
Heat and mass balance of MCFC–SCO_2 system.

State	T (K)	P (bar)	m (g s^{-1})	Composition (%v)						
				HC	H_2	H_2O	CO	CO_2	O_2	N_2
MCFC										
1	298	1	20.24	99.51	0	0	0	0	0	0.49
2	301.5	1.042	20.24	99.51	0	0	0	0	0	0.49
3	298	1.044	65.02	0	0	100	0	0	0	0
4	378.9	1.042	65.02	0	0	100	0	0	0	0
5	357.8	1.042	85.25	24.97	0	74.91	0	0	0	0.12
6	751.1	1.038	85.25	24.97	0	74.91	0	0	0	0.12
7	893	1.034	85.25	24.97	0	74.91	0	0	0	0.12
8	298	1	731.21	0	0	0	0	0.04	21.15	78.82
9	303	1.048	731.21	0	0	0	0	0.04	21.15	78.82
10	717	1.044	731.21	0	0	0	0	0.04	21.15	78.82
11	893	1.044	4161.62	0	0	16.76	0	3.51	11.44	68.29
12	923	1.024	3093.60	0	7.71	47.13	3.54	41.57	0	0.05
13	923	1.024	3937.45	0	0	17.40	0	1.09	10,60	70.90
14	982	1.016	4246.73	0	0	20.11	0	4.20	9.50	66.19
15	922.7	1.012	4246.73	0	0	20.11	0	4.20	9.50	66.19
16	922.7	1.012	3430.62	0	0	20.11	0	4.20	9.50	66.19
17	932.3	1.048	3430.62	0	0	20.11	0	4.20	9.50	66.19
18	925.3	1.044	3430.62	0	0	20.11	0	4.20	9.50	66.19
19	922.7	1.012	816.63	0	0	20.11	0	4.20	9.50	66.19
20	851.1	1.008	816.63	0	0	20.11	0	4.20	9.50	66.19
21	534.4	1.004	816.63	0	0	20.11	0	4.20	9.50	66.19
22	356.6	1	816.63	0	0	20.11	0	4.20	9.50	66.19
Cycle SCO_2										
A	308	75	1182.7	0	0	0	0	100	0	0
B	386.2	225	1182.7	0	0	0	0	100	0	0
C	702.1	223.9	1182.7	0	0	0	0	100	0	0
D	923	219.4	1182.7	0	0	0	0	100	0	0
E	789	76.9	1182.7	0	0	0	0	100	0	0
F	405.3	75.8	1182.7	0	0	0	0	100	0	0

Table 7
Heat and mass balance of MCFC–Air system.

State	T (K)	P (bar)	m (g s^{-1})	Composition (%v)						
				HC	H_2	H_2O	CO	CO_2	O_2	N_2
MCFC										
1	298	1	20.24	99.51	0	0	0	0	0	0.49
2	301.5	1.042	20.24	99.51	0	0	0	0	0	0.49
3	298	1.044	65.02	0	0	100	0	0	0	0
4	378.9	1.042	65.02	0	0	100	0	0	0	0
5	357.8	1.042	85.25	24.97	0	74.91	0	0	0	0.12
6	751.1	1.038	85.25	24.97	0	74.91	0	0	0	0.12
7	893	1.034	85.25	24.97	0	74.91	0	0	0	0.12
8	298	1	731.21	0	0	0	0	0.04	21.15	78.82
9	303	1.048	731.21	0	0	0	0	0.04	21.15	78.82
10	717	1.044	731.21	0	0	0	0	0.04	21.15	78.82
11	893	1.044	4161.62	0	0	16.76	0	3.51	11.44	68.29
12	923	1.024	3093.60	0	7.71	47.13	3.54	41.57	0	0.05
13	923	1.024	3937.45	0	0	17.40	0	1.09	10.60	70.90
14	982	1.016	4246.73	0	0	20.11	0	4.20	9.50	66.19
15	922.7	1.012	4246.73	0	0	20.11	0	4.20	9.50	66.19
16	922.7	1.012	3430.62	0	0	20.11	0	4.20	9.50	66.19
17	932.3	1.048	3430.62	0	0	20.11	0	4.20	9.50	66.19
18	925.3	1.044	3430.62	0	0	20.11	0	4.20	9.50	66.19
19	922.7	1.012	816.63	0	0	20.11	0	4.20	9.50	66.19
20	851.1	1.008	816.63	0	0	20.11	0	4.20	9.50	66.19
21	534.4	1.004	816.63	0	0	20.11	0	4.20	9.50	66.19
22	356.6	1	816.63	0	0	20.11	0	4.20	9.50	66.19
Cycle Air										
A	298	1	1402	0	0	0	0	0.03	20.95	78.08
B	434.6	3	1402	0	0	0	0	0.03	20.95	78.08
C	712.4	2.925	1402	0	0	0	0	0.03	20.95	78.08
D	923	2.866	1402	0	0	0	0	0.03	20.95	78.08
E	742.5	1.047	1402	0	0	0	0	0.03	20.95	78.08
F	466.2	1	1402	0	0	0	0	0.03	20.95	78.08

A similar behaviour is followed by the useful to expansion work ratio. As shown in Figs. 5 and 6, where the effect of turbine and compressor efficiencies on the aforementioned parameter is shown, Φ is more sensitive to η_c and η_t where air is used what adds up to the fact that both internal efficiencies are likely to be higher when supercritical carbon dioxide is employed. Overall, Φ takes typical values of 0.7 and 0.3+ for carbon dioxide and air respectively, this being a confirmation of the dramatic

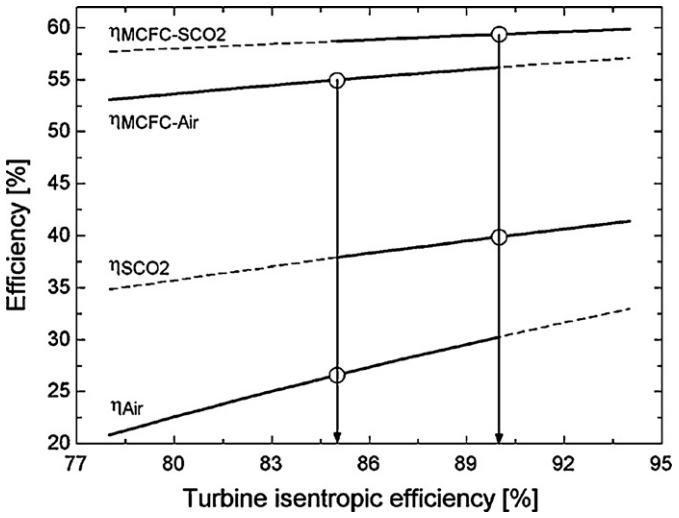

Fig. 3. Effect of turbine isentropic efficiency on hybrid and bottoming system efficiencies.

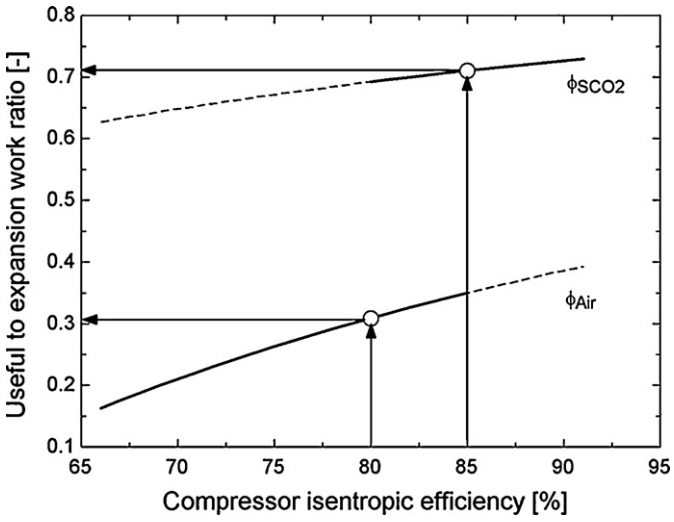

Fig. 6. Effect of compressor isentropic efficiency on useful to expansion work ratio.

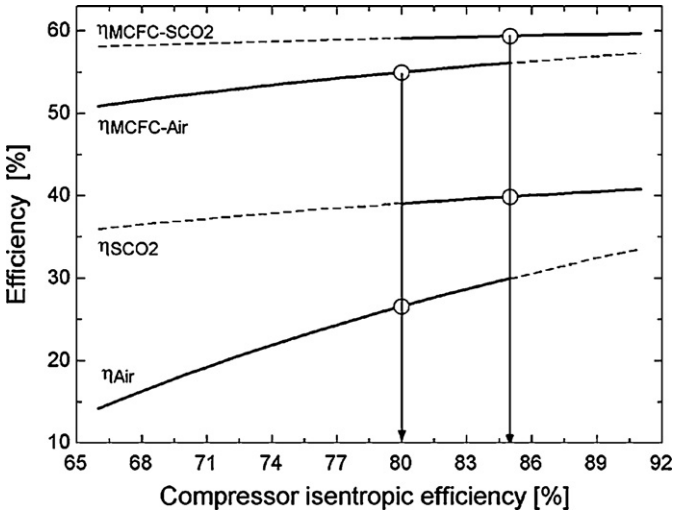

Fig. 4. Effect of compressor isentropic efficiency on hybrid and bottoming system efficiencies.

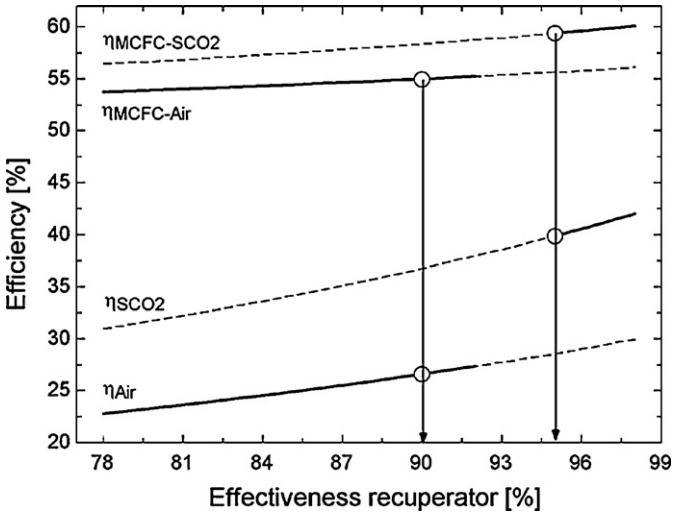

Fig. 7. Effect of recuperator effectiveness on hybrid and bottoming systems.

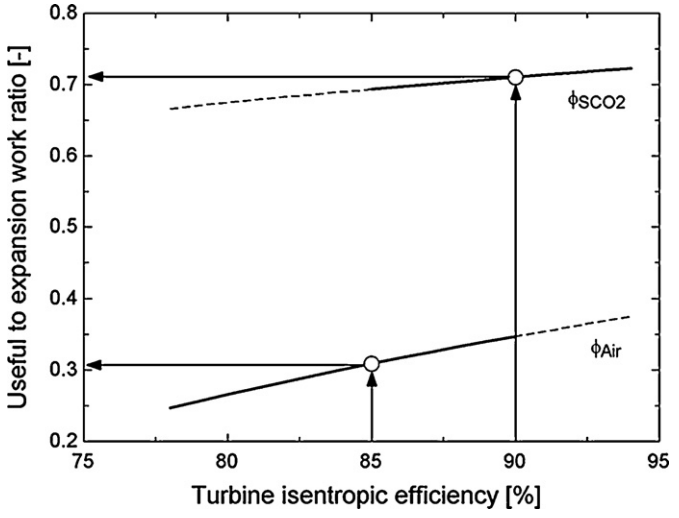

Fig. 5. Effect of turbine isentropic efficiency on useful to expansion work ratio.

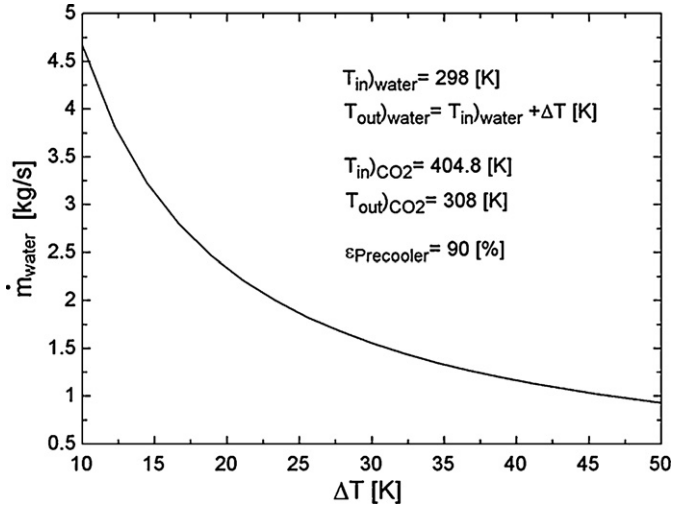

Fig. 8. Coolant requirement. Effect of temperature change on mass flow rate.

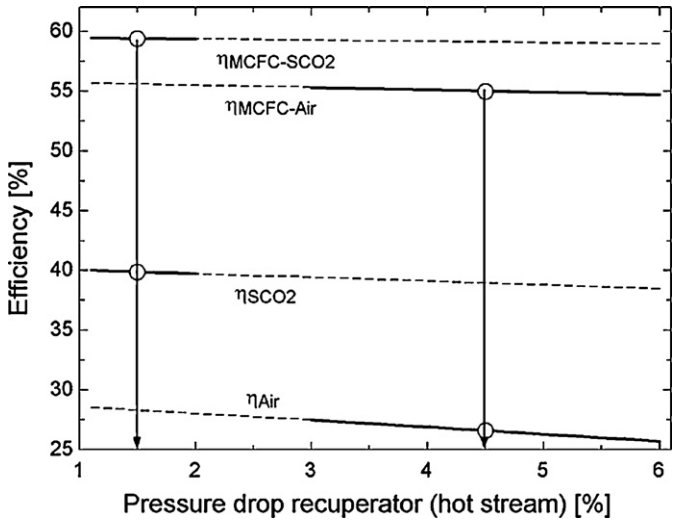

Fig. 9. Effect of hot side pressure loss at the recuperator on hybrid and bottoming systems.

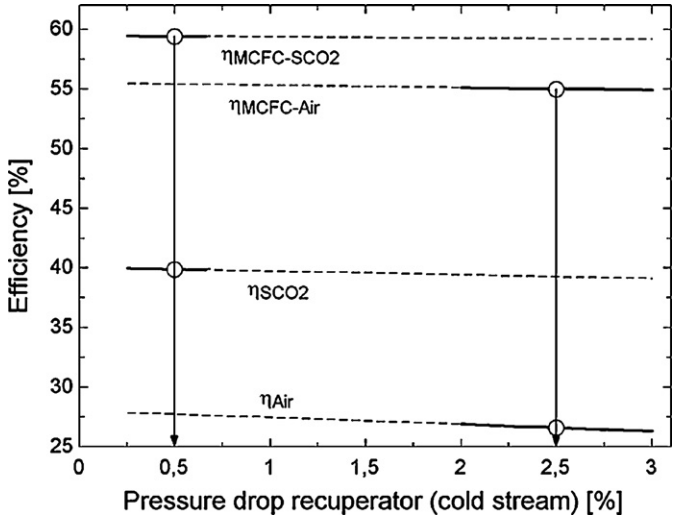

Fig. 10. Effect of cold side pressure loss at the recuperator on hybrid and bottoming systems.

decrease in compressor work achieved by the proposed system.

With respect to recuperator effectiveness, it is carbon dioxide that shows a higher sensitivity, what is easily deduced from the considerations exposed in Section 2. Thus, bottoming system efficiency changes 50% more for carbon dioxide than for air when this parameter varies between 78% and 98%. Nevertheless, this difference is attenuated at hybrid system level, for which both working fluids show somewhat similar performances. Results for the useful to expansion work ratio are not shown since there is little dependence of Φ on ε. On the contrary, it is interesting to note the direct link between the precooler, HX5 in Fig. 2, and the mass flow of water required to reduce the temperature of carbon dioxide down to its design value. This mass flow rate depends on the inlet temperature of both streams, heat exchanger effectiveness and allowable coolant temperature change. The first two operating/design conditions are set by other components of the plant (for instance the inlet temperature of carbon dioxide depends on recuperator performance) or by technology availability (HX5 effectiveness). The third one, coolant heating, is on the contrary constrained by environmental issues or by legislation directly. The rapid increase of water mass flow when its permissible temperature increase is reduced is plotted in Fig. 8, where the reference operating conditions are also indicated. Typical values of ΔT are higher than 25 K, yielding low water requirements. However, should hot water need to be returned at a lower temperature, parasitic losses due to pumping power would be not negligible.

Finally, with respect to pressure losses, both fluids, air and supercritical carbon dioxide, seem to be quite independent of this parameter and only the higher sensitive of air to the hot side pressure loss is worthy of note. The same behaviour is observed with regard to the useful to expansion work ratio, where Φ_{air} changes from 0.3 to 0.33 where Δp_{hot} changes from 6% to 3%. In this latter case, graphical results are not interesting and therefore are not provided.

In summary, two reasons are identified to be responsible for the different performance of hybrid systems using hot air and carbon dioxide. First, performance specifications of major equipments are not the same and, in some cases, differ significantly, Table 4. Second, the sensitivity of each cycle to variations of these performance specifications can be, for some parameters, very different.

5. Conclusions

This paper presents a proposal for increasing the efficiency of high temperature fuel cell and bottoming gas turbine hybrid systems orientated at systems where the fuel cell operates at atmospheric pressure. The system proposed is based on employing bottoming closed cycle gas turbines working with supercritical carbon dioxide as opposed to open cycle hot air turbines used in conventional hybrid systems. This concept emerges from the constraint imposed by fuel cell operating temperature on turbine inlet temperature and, therefore, turbine work. Accordingly, alternatives are sought to reduce compression work as much as possible in order to increase net useful work.

According to the results reported throughout the paper, the supercritical carbon dioxide based cycle meets these requirements, reducing compression work significantly to only 30% of the work generated at the turbine, for 60% of the hot air turbine. Additionally, after an ample literature review, it is observed that major equipments (turbine, compressor and recuperator) yield better performance when working with supercritical carbon dioxide rather than hot air.

Results of adding both effects show that MCFC–SCO_2 achieve 60% efficiency, what means a 10% increase with respect to conventional systems using hot air turbines, even if equipment capable of withstanding very high pressure and temperature is required. Nevertheless, this latter aspect of supercritical carbon dioxide seems to be not a problem for state of the art technology according to the numerous references provided throughout the text (i.e. applications using similar operating conditions are currently being used in industry).

References

[1] S. McPhail, A. Moreno, R. Bove, International status of molten carbonate fuel cell (MCFC) technology, ENEA Report RSE/2009/181, 2008.
[2] K. Kordesch, G. Simader, Fuel Cells and Their Applications, Wiley-VCH, 1996.
[3] D. Sánchez, R. Chacartegui, A. Muñoz, T. Sánchez, Proceedings of the ASME Turbo Expo 2008, Berlin, 2008.
[4] D. Sánchez, R. Chacartegui, F. Jiménez Espadafor, T. Sánchez, J. Fuel Cell Sci. Technol. 6 (2009) 021306.
[5] S.R. Turns, Thermodynamics Concepts and Applications, Cambridge University Press, New York, 2006.
[6] S. Kakaç, H. Liu, Heat Exchangers: Selection, Rating and Thermal Design, CRC Press, Boca Raton, 2002.
[7] A.F. Massardo, C.F. McDonald, T. Korakianitis, J. Eng. Gas Turbines Power-Trans. ASME 124 (2002) 110–116.
[8] G. Lagerstrom, M. Xie, Proceedings of the ASME Turbo Expo 2002, Amsterdam, 2002.

[9] D. Micheli, V. Pediroda, S. Pieri, J. Eng. Gas Turbines Power-Trans. ASME 130 (2008) 032301.
[10] W. Qiuwang, L. Hongxia, X. Gongnan, Z. Min, L. Laiqin, F.Z. Ping, J. Eng. Gas Turbines Power-Trans. ASME 129 (2007) 436–442.
[11] S. Campanari, L. Boncompagni, E. Macchi, J. Eng. Gas Turbines Power-Trans. ASME 126 (2004) 92–101.
[12] E. Utriainen, B. Sundén, J. Eng. Gas Turbines Power-Trans. ASME 124 (2002) 550–560.
[13] S. Campanari, J. Eng. Gas Turbines Power-Trans. ASME 122 (2000) 239–246.
[14] J. Kaikko, J. Backman, Energy 32 (2007) 378–387.
[15] E. Benini, A. Toffolo, A. Lazzaretto, Exp. Therm. Fluid Sci. 30 (2006) 427–440.
[16] P. Akbari, R. Nalim, N. Müller, J. Eng. Gas Turbines Power-Trans. 128 (2006) 190–202.
[17] T. Stevens, M. Baelmans, Appl. Therm. Eng. 28 (2008) 2353–2359.
[18] M.J. Moore, Micro-turbine Generators, Professional Engineering Publishing, Bury St Edmunds-London, 2002.
[19] S. Velumani, C.E. Guzmán, R. Peniche, R. Vega, Int. J. Energy Res. (2009), doi:10.1002/er.
[20] K. Wana, S. Zhanga, J. Wanga, Y. Xiao, Energy Convers. Manage., in press, doi:10.1016/j.enconman.2010.03.005.
[21] C.F. McDonald, Appl. Therm. Eng. 23 (2003) 1463–1487.
[22] E. Benini, S. Giacometti, Appl. Energy 84 (2007) 1102–1116.
[23] V. Verda, F. Nicolin, Int. J. Hydrogen Energy 35 (2010) 794–806.
[24] A.V. Akkaya, B. Sahinb, H.H. Erdem, Int. J. Hydrogen Energy 33 (2008) 2566–2577.
[25] Y. Haseli, I. Dincer, G.F. Naterer, Int. J. Hydrogen Energy 33 (2008) 5811–5822.
[26] P. Greppi, B. Bosio, E. Arato, Int. J. Hydrogen Energy 33 (2008) 6327–6338.
[27] Modeling of Combined SOFC and Turbine Power Systems. Methods, Procedures and Techniques. Springer, Netherlands, 2008 (libro).
[28] V. Cenusa, F. Alexe, Wseas Transactions on Environment and Development, Issue 4, Volume 3, April 2007.
[29] J. Kesseli, T. Wolf, J. Nash, S.J. Freedman, Proceedings of the ASME Turbo Expo 2003, Atlanta, 2003.
[30] R.K. Shah, Proceedings of the 5th International Conference on Enhanced, Compact and Ultra-Compact Heat Exchangers, Hoboken, 2005.
[31] Y. Komatsu, S. Kimijima, J.S. Szmyd, Energy 35 (2010) 982–988.
[32] S. Specchia, G. Saracco, V. Specchia, Int. J. Hydrogen Energy 33 (2008) 3393–3401.
[33] Technology Characterization: Microturbines, Energy Nexus Group, 2002.
[34] C. Soares, Microturbines, Buterworth-Heinemann, Burlington, 2007.
[35] Recuperators for Gas Turbine Engines. Ingersoll Rand Inc. (www.irenergysystems.com).
[36] A. Traverso, A.F. Massardo, Appl. Therm. Eng. 25 (2005) 2054–2071.
[37] C.F. McDonald, C. Rodgers, Appl. Therm. Eng. 28 (2008) 60–74.
[38] J.P. Gibbs, Power conversion system design for supercritical carbon dioxide cooled indirect cycle nuclear reactors, MSc. Thesis, Massachusetts Institute of Technology, 2008.
[39] Y. Gong, N.A. Carstens, M.J. Driscoll, I.A. Matthews, Analysis of radial compressor options for supercritical CO_2 power conversion cycles, MIT Topical Report MIT-GFR-034, 2006.
[40] A.R. Ludington, Tools for supercritical carbon dioxide cycle analysis and the cycle's applicability to sodium fast reactors, MSc. Thesis, Massachusetts Institute of Technology, 2009.
[41] J.E. Cha, T.H. Lee, J.H. Eoh, S.H. Seong, S.O. Kim, D.E. Kim, M.H. Kim, T.W. Kim, K.Y. Suh, Nucl. Eng. Technol. 41 (8) (2009) 1025–1044.
[42] N.A. Carstens, Control strategies for supercritical carbon dioxide power conversion systems, ScD Thesis, Massachusetts Institute of Technology, 2007.
[43] T.Q. Trinh, Small scale closed Brayton cycle recompression cycle to various system transients, MSc. Thesis, Massachusetts Institute of Technology, 2009.
[44] Y. Muto, Y. Kato, JSME J. Power Energy Syst. 2 (3) (2008) 1060–1073.
[45] Y. Kato, T. Nitawaki, Y. Muto, Nucl. Eng. Des. 230 (2004) 195–207.
[46] J.P. Gibbs, P. Hejzlar, M.J. Driscoll, Applicability of supercritical CO_2 power conversion systems to GEN IV reactors, MIT Topical Report MIT-GFR-037, 2006.
[47] V. Dostal, M.J. Driscoll, P. Hejzlar, A supercritical carbon dioxide cycle for next generation nuclear reactors, MIT Topical Report MIT-ANPTR-100, 2004.
[48] J. Sarkar, S. Bhattacharyya, Energy Convers. Manage. 50 (2009) 1939–1945.
[49] M. Schleer, S.S. Hong, M. Zangeneh, C. Roduner, B. Ribi, F. Pløger, R.S. Abhari, J. Turbomach.-Trans. ASME 126 (2004) 82–90.
[50] J.K. Min, J.H. Jeong, M.Y. Ha, K.S. Kim, Heat Mass Transfer 46 (2009) 175–186.
[51] C.H. Oh, T. Lillo, W. Windes, T. Totemeier, R. Moore, Development of a Supercritical Carbon Dioxide Brayton Cycle: Improving PBR Efficiency and Testing Material Compatibility, Idaho National Engineering and Environmental Laboratory INEEL/EXT-04-02437, 2004.
[52] C.H. Oh, T. Lillo, W. Windes, T. Totemeier, R. Moore, R. Barner, Development of a Supercritical Carbon Dioxide Brayton Cycle: Improving VHTR Efficiency and Testing Material Compatibility, Idaho National Engineering and Environmental Laboratory INL/EXT-06-01271, 2006.
[53] N.A. Carstens, P. Hejzlar, M.J. Driscoll, Control system strategies and dynamic response for supercritical CO_2 power conversion cycles, MIT Topical Report MIT-GFR-038, 2006.